Analysis and Experimental Results of Switched-Resonator-Based Buck-Boost and Inverting-Buck Converters

M. Jabbari, and H. Farzanefard
Elect. and Comp. dept., Isfahan university of technology, 84154, Isfahan, Iran

***Abstract*-- Two resonant DC-DC converters are presented where an LC tank is switched by an inverter. One of the presented topologies is buck-boost and the other one is inverting-buck converter. Few numbers of elements are employed, turn-on and turn-off ZCS conditions are provided for all active elements, energy circulation is reduced, and, power transferring is automatically stopped at output short-circuited. Experimental results from a 200W laboratory prototype confirm the presented theoretical analysis.**

***Index Terms*-- resonant converter, soft switching, ZCS, buck-boost converter, inverting-buck converter.**

I. INTRODUCTION

Soft-switching converters have been widely employed for DC-DC power conversion because at soft-switching conditions switching losses and electromagnetic interference (EMI) are reduced. Moreover, switching frequency can be increased to enhance the converter power density. This condition is commonly attained by zero-voltage switching (ZVS) or zero current-switching (ZCS) [1]-[19].

Resonant converters are a family of soft-switching converters in which energy is transferred through a high-frequency resonant tank, and switching is performed at zero-crossing instants of the switches current or voltage. A series resonant LC tank is the simplest network which is employed in the resonant converters to provide ZCS [1]-[7]. The main advantage of this converter (series resonant converter, SRC) is major size reduction of the passive components. With this method, complete ZCS condition is attained at discontinues conduction mode, DCM ($f_S<f_r/2$), where even by a full-bridge inverter voltage gain greater than unity cannot be achieved [1], [5]. Further resonant networks such as LLC, LCC, etc. are also proposed however the number of elements is increased and the system possesses complicated characteristics [11]-[18]. As a non-isolated converter, a restriction of the conventional resonant converters is the requirement of a full-wave rectifier which detaches the common ground of the load and source. This is in addition to the increased number elements and conduction losses.

A new family of resonant converters so-called switched-resonator converters is proposed in [7]. Based on the mentioned general scheme in [7], this paper presents analysis of a resonant step down/up converter shown in Fig. 1. In this converter, namely buck-boost-MG, similar to the SRC, passive components include a high frequency resonant tank and a filtering capacitor at the output. A half-bridge inverter is employed, and ZCS condition is achieved at both turn on and turn off switching instants independent of the load-current and operating voltages. The diode operates at ZVS, and the converter operation is automatically stopped at output short-circuited. Comparing with the HB-SRC, not only the proposed converter has three power diodes less, but also it is suitable for non-isolated applications and voltage gain greater than unity is attainable. Since the switches are unidirectional, current cannot return to the source and thus no reactive power is created in view of the voltage source.

II. ANALYSIS OF PROPOSED BUCK-BOOST CONVERTER

Topology of the proposed buck-boost converter is shown in Fig. 1. According to the direction of diode D_r, the voltage gain of this converter is negative similar to its PWM counterpart. Equivalent circuit of each operating mode and steady-state waveforms are shown in Figs. 2 and 3 respectively. Following quantities are defined.

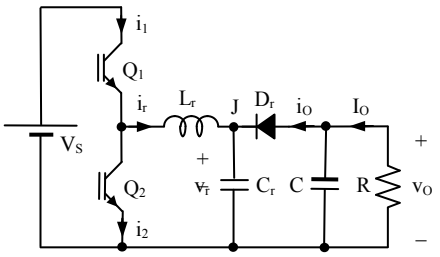

Fig. 1 – Proposed buck-boost converter topology

$$\omega_r = 1/\sqrt{L_r C_r}\ ,\quad f_r = 1/T = \omega_r/(2\pi) \tag{1}$$

$$Z_r = \sqrt{L_r/C_r} \tag{2}$$

$$r = R/Z_r \tag{3}$$

$$A = |V_O|/V_S \tag{4}$$

Assume that prior to Mode I, the resonant voltage v_r is

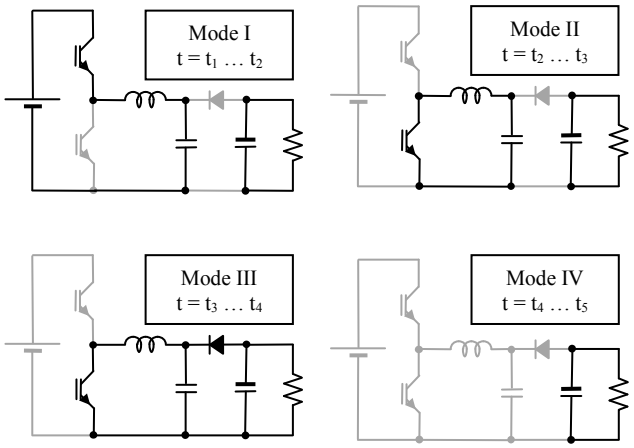

Fig. 2 – Equivalent circuits of the proposed buck-boost converter

V_O (V_O in negative), resonant current i_r is zero, and Q_1 and Q_2 are off. To simplify the analysis, all the circuit elements are assumed ideal and the capacitor C is considered large enough such that the output voltage is constant during one switching cycle. The converter operates in four modes as following.

Mode I (t_1 – t_2): At t_1, Q_1 is turned on at ZCS and C_r charges through a resonance with L_r. At t_2 the resonant current reaches zero and thereby Q_1 is turned off at ZCS.

$$\frac{v_r(t)}{V_S} = 1 - (1+A)\cos\left(\omega_r \cdot (t - t_1)\right) \tag{5}$$

$$\frac{i_r(t)}{V_S / Z_r} = (1+A)\sin\left(\omega_r \cdot (t - t_1)\right) \tag{6}$$

$$t_2 - t_1 = \pi / \omega_r \tag{7}$$

Mode II (t_2 – t_3): At t_2, Q_2 is turned on at ZCS and the voltage polarity of C_r starts reversing through a resonance with L_r. At t_2, v_r reaches V_O and thereby D_r becomes forward biased.

$$\frac{v_r(t)}{V_S} = (2+A)\cos\left(\omega_r \cdot (t - t_2)\right) \tag{8}$$

$$\frac{i_r(t)}{V_S / Z_r} = -(2+A)\sin\left(\omega_r \cdot (t - t_2)\right) \tag{9}$$

$$t_3 - t_2 = \frac{1}{\omega_r}\left[\pi - \cos^{-1}\frac{A}{2+A}\right] \tag{10}$$

$$\frac{i_r(t_3)}{V_S / Z_r} = \frac{i_{D_r,\max}}{V_S / Z_r} = 2\sqrt{1+A} \tag{11}$$

Mode III (t_3 – t_4): At t_3, D_r turns on at ZVS and the resonant current continues through it. Since C is much larger than C_r, voltage of node J (see Fig. 1) is constant and equal to V_O during this mode. Thus magnitude of i_r decreases linearly until at t_4 it reaches zero. At this instant, both Q_2 and D_r are turned off at ZCS.

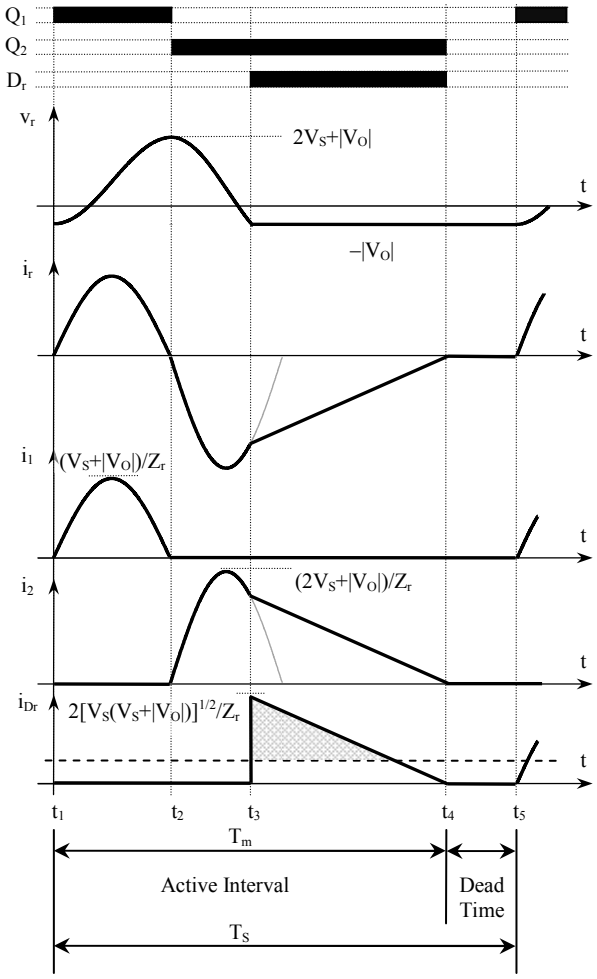

Fig. 3 – Key waveforms of the proposed buck converter

$$\frac{v_r(t)}{V_S} = -A \tag{12}$$

$$\frac{i_r(t)}{V_S / Z_r} = -2\sqrt{1+A} + A\,\omega_r\,(t - t_3) \tag{13}$$

$$t_4 - t_3 = \frac{1}{\omega_r}\frac{2\sqrt{1+A}}{A} \tag{14}$$

Mode IV (t_4 – t_5): In this mode, Q_1 and Q_2 are both off and the load is supplied by the output capacitor. Duration of this interval is determined by the controller so that proper voltage regulation is attained (dead-time control).

III. Voltage Gain

At steady-state, the converter voltage gain A is calculated by satisfying the energy conservation principle in one switching cycle.

$$\int_{T_S} V_S\, i_1\, dt = \int_{T_S} \frac{V_O^2}{R} dt \tag{15}$$

Where $f_S = T_S^{-1}$ is the switching frequency. By substituting (6) in (15), voltage gain is obtained from (16)

where S is defined by (17).

$$S = \frac{A^2}{1+A} \tag{16}$$

$$S = 2RC_r f_S = \frac{r}{\pi} \times \frac{f_S}{f_r} \tag{17}$$

In absence of dead-time (Mode IV), the converter operates at its maximum power handling capability where the switching frequency is also at maximum. This situation is named maximum power delivery condition. The interval from t_1 to t_4 is defined as T_m (see Fig. 3). By using (7), (10) and (14), (18) is obtained.

$$\frac{T_m}{T_r} = 1 + \frac{1}{\pi}\left[\frac{\sqrt{1+A}}{A} - \frac{1}{2}\cos^{-1}\frac{A}{2+A}\right] \tag{18}$$

By substituting (18) in (17) and after a few calculations, (19) is attained. This equation gives maximum attainable voltage gain, A_m, versus r.

$$r = \frac{A_m^2}{1+A_m} \cdot \left[\pi + \frac{\sqrt{1+A_m}}{A_m} - \frac{1}{2}\cos^{-1}\frac{A_m}{2+A_m}\right] \tag{19}$$

At output short-circuited, A is zero and thus according to (18) T_m goes infinity. Since T_m is the shortest switching period, power transferring is automatically stopped when the output is short-circuited.

IV. Proposed Inverting-Buck Converter

As shown in Fig. 4, Q_2 can be replaced with a bidirectional switch. Consequently, as shown in Fig. 5, another mode is added in which during t_4 to t_5 the anti-parallel diode of Q_2 reverses v_r through a resonance. Modal analysis of this converter is very similar to that of the pervious converter and the important values are mentioned on Fig. 5. The essential relations of this converter are as following.

$$S = \frac{A^2}{1-A} \tag{20}$$

$$r = \frac{A_m^2}{1-A_m} \cdot \left[\frac{3\pi}{4} + \frac{\sqrt{1-A_m}}{A_m} - \frac{1}{2}\cos^{-1}\frac{A_m}{2-A_m}\right] \tag{21}$$

According to (21), voltage gain of this converter is limited to unity and hence topology of Fig. 5 is an inverting-buck converter. The switch Q_2 is turned on at ZCS as well, but now is turned off at ZVZCS. Similar to HB-SRC, this converter can operate at continues conduction mode (CCM) to increase voltage gain. However, in both converters, CCM leads to hard-switching operation at either turn on or turn off instant.

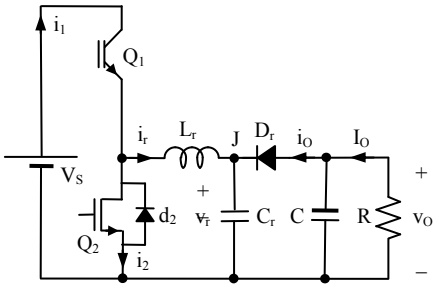

Fig. 4 – Proposed inverting-buck converter topology

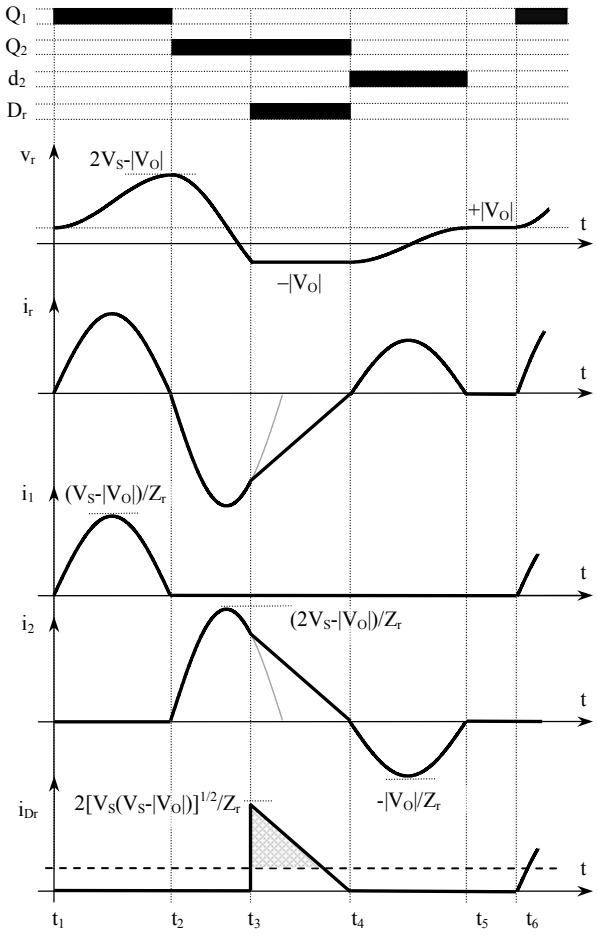

Fig. 5 – Key waveforms of the proposed inverting-buck converter

V. Performance Analysis

The peak-to-peak output voltage ripple ΔV_O is calculated approximately assuming that the ripple component is entirely absorbed by the output capacitor and its DC part flows through the load [1]. The shaded areas in Figs. 3 and 5 represent additional charges that produce the ripple components. After a few calculations the output voltage ripple is obtained as (22).

The converters efficiency η is calculated from (23) where V_D is the diode forward voltage, V_F is the switch drop voltage, R_{ON} is on resistance, and R_r is the parasitic resistance of L_r. Equations (24) are the result of curve-fitting.

$$\frac{\Delta V_O}{V_O}=\frac{C_r}{2C}\times\begin{cases}\left(\dfrac{2\sqrt{1+A}}{A}-\dfrac{1}{r}\right)^2 & \text{Buck-boost}\\ \left(\dfrac{2\sqrt{1-A}}{A}-\dfrac{1}{r}\right)^2 & \text{Buck}\end{cases} \tag{22}$$

$$\frac{1}{\eta}=\begin{cases}1+\dfrac{V_D}{|V_O|}+\dfrac{V_F}{|V_O|}(2A+1)+\dfrac{R_{ON}+R_r}{Z_r}\rho & \text{Buck-boost}\\ 1+\dfrac{V_D}{|V_O|}\left(1+\dfrac{A^2}{1-A}\right)+\dfrac{R_{ON}+R_r}{Z_r}\rho & \text{Buck}\end{cases} \tag{23}$$

$$\rho=\begin{cases}\dfrac{1.573A^2+3.088A+1.325}{A} & \text{Buck-boost}\\ \dfrac{1.627A^2-3.401A+2.382}{1-A} & \text{Buck}\end{cases} \tag{24}$$

It can be proven that when the converters efficiency is taken into account, relations of voltage gain are obtained from (16) and (20) by substituting $S\rightarrow\eta S$. For both proposed converters, A_m versus r/π is plotted in Fig. 6.

Voltage and current stresses of the active elements are presented in Table I. According to this table, the switches reverse voltage stresses (maximum of V_{EC}) is always less than or equal to the forward voltage stresses (maximum of V_{CE}). As a result, voltage rating of the switches is determined by the maximum of forward voltage the same as that of the bidirectional switches.

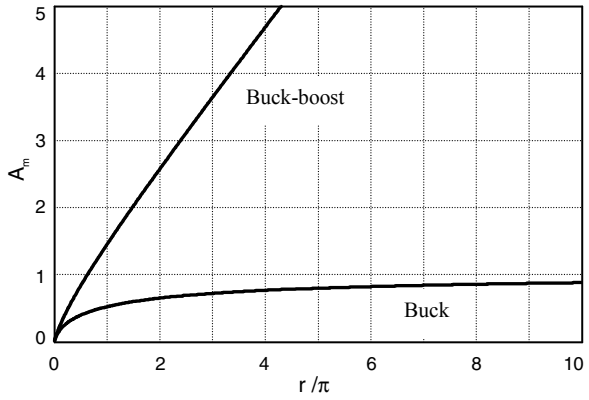

Fig. 6 – Maximum attainable voltage gain A_m versus r/π

TABLE I
VOLTAGE AND CURRENT STRESSES

Element	Buck			Buck-boost		
	Voltage Stresses[1]		Current Stress[2]	Voltage Stresses[1]		Current Stress[2]
	Forward	Reverse		Forward	Reverse	
Q_1	1	0 or 1-A	1-A	1+A	1+A	1+A
Q_2	2-A	0	2-A	2+A	A	2+A
D_r	-	2	$2(1-A)^{0.5}$	-	2(1+A)	$2(1+A)^{0.5}$

[1] Normalized to V_S [2] Normalized to V_S/Z_r

VI. EXPERIMENTAL RESULTS

The prototype is a 200W buck-boost converter for V_S=100..170V to V_O=156V, f_r=167KHz, and ΔV_O<2%. With 20% overdesign, the circuit elements are calculated as L_r=29μH, C_r=32nF, and C=9μF. The switches and diodes are STY30NK90 and MUR880. For V_S=160V, the experimental waveforms are presented in Fig. 7. Guidelines of [19] can be employed to reduce additional voltage stresses created due to oscillations of the switch output capacitance with L_r. The measured efficiency curve is illustrated in Fig. 8.

VII. CONCLUSIONS

A buck-boost and an inverting buck converter are presented where a simple LC resonant tank is the middle of energy transfer. Few numbers of elements are employed, fully soft-switching operation is attained, voltage gain is adjustable, and self output short-circuit protection is achieved. Experimental results from a 200W laboratory prototype confirm the presented theoretical analysis.

REFERENCES

[1] N. Mohan, T.M. Undeland, and W.P. Robbins, *Power Electronics: Converters, Applications, and Design*, 3rd ed., John Wiley & Sons, 2002.

[2] J. Abu-Qahouq, and I. Batarseh, "Unified steady-state analysis of soft switching DC-DC converters," *IEEE Trans. on Power Electron.*, vol. 17, no. 5, pp. 684–691, Sep. 2002.

[3] EE. Buchanan, and E.J. Miller, "Resonant switching power conversion technique," *IEEE Power Electronics Specialists Conference*, 1975, pp. 188-193.

[4] R. Oruganti, and F.C. Lee, "Resonant power processor: Part I - State plain analysis," *IEEE-IAS '84 Annual Meeting*, pp. 860-867.

[5] R.L. Steigerwald, "A comparison of half-bridge resonant converter topologies," *IEEE Trans. on Power Electron.*, 1988, 3, (2), pp. 174–182.

[6] C.H. Kang, H. Sakamoto, K. Harada, and H.J. Kim, "A half-bridge converter using series-resonant technology and saturable inductor commutation," *IEEE PESC'01*, vol. 2, 2001, pp. 1051-1056.

[7] M. Jabbari, and H. Farzanehfard, "Family of Soft Switching Resonant DC-DC converters," *IET Power Electron., 2009*, Vol. 2, Iss. 2, pp. 113–124.

[8] T. Zheng, D.Y. Chen, and F.C. Lee, "Variation of quasi resonant DC/DC converter topologies," *in Proc. IEEE Power Electron. Spec. Conf.*, 1986, pp. 381–392.

[9] K.-H. Liu, R. Oruganti, and F.C. Lee, "Quasiresonant converters – Topologies and characteristics," *IEEE Trans. on Power Electron.*, vol. 2, no. 1, pp. 62–71, 1987.

[10] D. Maksimovic, and S. Cuk, "A general approach to synthesis and analysis of quasi-resonant converters," *IEEE Trans. on Power Electron.*, Vol. 6, no. 1, pp. 127-140, Jan. 1991.

[11] A.K.S. Bhat, "Analysis and design of a series-parallel resonant converter," *IEEE Trans. on Power Electron.*, vol. 8, no 1, pp. 1-11, Jan. 1993.

[12] F. Dianbo, F.C. Lee, L. Ya, and X. Ming, "Novel multi-element resonant converters for front-end dc/dc converters," *IEEE PESC'08*, June 2008, pp. 250-256.
[13] M. Borage, S. Tiwari, and S. Kotaiah, "LCL-T resonant converter with clamp diodes: a novel constant-current power supply with inherent constant-voltage limit," *IEEE Trans. Ind. Elect.*, vol. 54, no. 2, April 2007, pp. 741-746.
[14] X. Xie, J. Zhang, C. Zhao, Z. Zhao, and Z. Qian, "Analysis and optimization of LLC resonant converter with a novel over-current protection circuit," *IEEE Trans. on Power Electron.*, vol. 22, no. 2, March 2007, pp. 435-443.
[15] M.Z. Youssef, and P.K. Jain, "Series–parallel resonant converter in self-sustained oscillation mode with the high-frequency transformer-leakage-inductance effect: analysis, modeling, and design," *IEEE Trans. on Ind. Electron.*, vol. 54, no. 3, June 2007, pp. 1329-1341.
[16] J.A. Martín-Ramos, J. Díaz, A.M. Pernía, J. M. Lopera, and F. Nuño, "Dynamic and steady-state models for the PRC-LCC resonant topology with a capacitor as output filter", *IEEE Trans. on Ind. Electron.*, vol. 54, no. 4, August 2007, pp. 2262-2275.
[17] S. Zheng, and D. Czarkowski, "Modeling and digital control of a phase-controlled series–parallel resonant converter," *IEEE Trans. on Ind. Electron.*, vol. 54, no. 2, April 2007, pp. 707-715.
[18] M.P. Foster, C.R. Gould, A.J. Gilbert, D.A. Stone, and C.M. Bingham, "Analysis of CLL voltage-output resonant converters using describing functions," *IEEE Trans. on Power Electron.*, vol. 23, no. 4, July 2008, pp. 1772-1781.
[19] G. Ivensky, I. Zeltser, A. Kats, and S. Ben-Yaakov, "Reducing IGBT losses in ZCS series resonant converters," *IEEE Trans. on Ind. Electron.*, vol. 46, no. 1, Feb 1999.

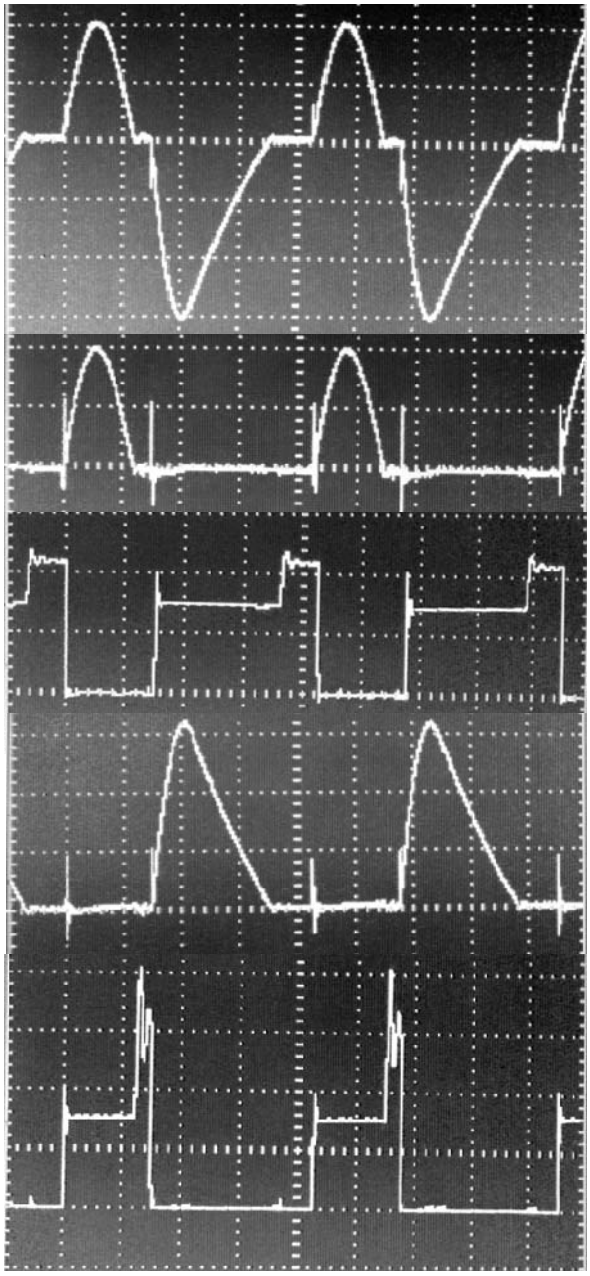

Fig. 7 – Soft-switching operation of the converter, respectively from the top: i_r, Q_1 current, Q_1 voltage, Q_2 current, Q_2 voltage, 10A/div, 200V/div, 2.5µs/div

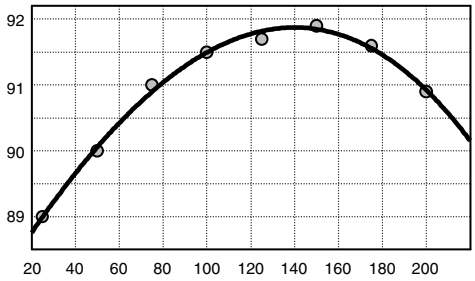

Fig. 8 – Efficiency (%) vs. output power (W)